Composite Structures **25** (1993) 547–555

A damage mechanics tool for laminate delamination

L. Daudeville & P. Ladevèze

Laboratoire de Mécanique et Technologie, ENS de Cachan/CNRS/Univ. P. et M. Curie, 61 avenue du Président Wilson, 94235 Cachan Cedex, France

A simplified method based upon damage mechanics for the delamination analysis of carbon–resin composites is presented. In the neighbourhood of a laminate structure quasi-straight edge, damage is taken concentrated on the interface between layers. The finite element code EDA, acting as a post-processor of an elastic laminate shell computation, allows the onset and propagation forecast of delamination. First numerical simulations of delamination are given and compared with experimental results from literature.

1 INTRODUCTION

The degradation modes of carbon–resin laminates (e.g. T300-914) can be split into two classes. On the one hand, intralaminar damages: transverse matrix cracking, fibre–matrix debonding, fibre ruptures. On the other hand, delamination, i.e. degradation of the link between layers. Laminate structures being thin (plates or shells), the stress state far away from the edge zones (free edges, zones of force application) is a plane stress state, whereas the stress state can be three-dimensional in the edge zones. Thus, delamination, a phenomenon of layer debonding due to possible stresses that are normal to the shell surface, occurs principally in the edge zones of laminate structures.

Numerical rupture simulation of a laminate structure, taking into account all the progressive degradation phenomena, leads to a time dependent three-dimensional non-linear problem. Nowadays, finite element calcualtions under a classical laminate theory and combined with stress criteria,[1] are generally used for the rupture forecast far away from the edge zones. Such an approach can be discussed because such criteria cannot well describe the different damage phenomena.

For the delamination analysis, more especially for the onset forecast of a free edge crack, computation methods of elastic edge effects[2–4] are generally used as post-processors of an elastic laminate shell computation. They are associated to criteria based upon the average of normal stresses along a characteristic distance from the free edge.[5] Progressive degradations are not yet taken into account. In addition, delamination does not always occur where stresses are maxima and the intrinsic feature of the distance from the free edge can be discussed when geometry and stacking sequence vary. Linear fracture mechanics, i.e. computation of an energy release rate G and its comparison with a critical value G_c, is generally used for crack propagation study.[6–8] Nevertheless, fracture mechanics cannot be used for crack onset study.

Progressive degradation modelling allows one to predict accurately the structure behaviour until rupture: that is damage mechanics of composites.[9–11] Numerical methods based upon damage mechanics proposed by Ladevèze,[11] acting as post-processors of an elastic laminate shell computation have been developed for the forecast of (i) rupture far away from the edge, (ii) rupture in the vicinity of a circular hole, and (iii) delamination near a quasi-straight edge.

Method (iii) is presented. The general ideas of that computational tool were first presented in Ref. 12. We present now the development and the first results of this simplified method that allows the forecast of delamination onset and its propagation on a short distance. Damage phenomena are taken concentrated on the interfaces between the layers. The edge is quasi-straight, thus the

Composite Structures 0263-8223/93/$06.00

initial three-dimensional problem becomes a two-dimensional one set into a band perpendicular to the edge.

The laminate is modelled as a stacking of homogeneous elastic layers connected by elastic with damage interfaces. The interface is a two-dimensional entity which ensures stress and displacement transfers between layers. The degradation effect is taken into account through the relative variations of the interface elastic moduli. An interface with damage has also been used recently by Schellekens[13] for delamination simulation of a laminate under tension. The interface modelling of this author is principally based upon numerical considerations. The interface modelling we propose has already been presented. In the previous presentation,[14] for the particular example of a double cantilever beam (DCB), a link has been established between damage mechanics of the interface and fracture mechanics giving a mechanical interpretation to that modelling. Note that the crack length was considered large compared with the beam thickness. In the present paper, the numerical simulation of the DCB test is performed with no initial crack. The finite element method is used. Due to damage, the structure may present a critical state. A method[15,16] in which crack opening displacement is controlled, allows such a limit point to be passed.

Numerical simulations of delamination, computed with the post-processor edge damage analysis (EDA), are given in the framework of (i) a DCB beam: study of onset and propagation of delamination, and (ii) a specimen under tension: study of delamination onset near the free edge. The proposed numerical simulations allow a comparison with experimental results from literature for the identification and the checking of the modelling.

2 DELAMINATION ANALYSIS BY DAMAGE MECHANICS

2.1 Laminate modelling

The laminate is modelled as a stacking (i) of homogeneous layers, and (ii) of interfaces connecting layers (see Fig. 1).

All damage phenomena are taken concentrated on the interface. The principal features of the interface are as listed below.

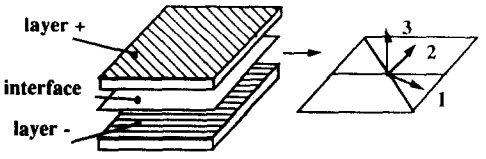

Fig. 1. Interface.

- *Its behaviour is assumed orthotropic* — the influence of the adjacent layers on the interface damage behaviour is taken into account through the fibre direction bisectors that are supposed to be the directions of orthotropy. The constitutive law links the normal stresses to the jump of displacement between layers, its expression in elasticity is

$$\begin{pmatrix} \sigma_{13} \\ \sigma_{23} \\ \sigma_{33} \end{pmatrix} = \begin{pmatrix} k_1^0 & 0 & 0 \\ 0 & k_2^0 & 0 \\ 0 & 0 & k^0 \end{pmatrix} \begin{pmatrix} [u_1] \\ [u_2] \\ [u_3] \end{pmatrix}$$

with

$$\begin{cases} [\mathbf{U}] = \mathbf{U}^+ - \mathbf{U}^- = [u_1]\mathbf{N}_1 + [u_2]\mathbf{N}_2 + [u_3]\mathbf{N}_3 \\ \text{jump of displacement between the + and } - \text{ layers} \end{cases}$$

Note the particular cases:

$$\begin{cases} k_1^0 = k_2^0 = k_3^0 = 0 \\ \quad \text{complete debonding between layers} \\ k_1^0 = k_2^0 = k_3^0 = \infty \\ \quad \text{perfect bonding} \end{cases}$$

- *Damage is unilateral in the 3 direction* — for the normal to the shell direction (mode *I*) there is no damage under compression.
- *Relative variations of stiffness are the damage indicators* — three internal variables d_i are associated to the three stiffness moduli k_i^0.
- *The interface behaviour is assumed to be elastic with damage* — that is at first, an inelastic behavour can also be introduced.[17]

The thermodynamical potential is the strain energy:

$$E_D = \frac{1}{2}\left(\frac{\langle -\sigma_{33} \rangle_+^2}{k_3^0} + \frac{\langle \sigma_{33} \rangle_+^2}{k_3^0(1-d_3)} + \frac{\sigma_{31}^2}{k_1^0(1-d_1)} + \frac{\sigma_{32}^2}{k_2^0(1-d_2)} \right)$$

$\langle \cdot \rangle_+$ denotes the positive part.

The variables Y_{di}, that are similar to the energy release rate introduced in fracture mechanics, are conjugated to d_i: $Y_{di} = \partial E_D / \partial d_i$

$$Y_{d1} = \frac{1}{2} \frac{\sigma_{31}^2}{k_1^0 (1-d_1)^2} \quad ; \quad Y_{d2} = \frac{1}{2} \frac{\sigma_{32}^2}{k_2^0 (1-d_2)^2} \quad ;$$

mode 1 mode 2

$$Y_{d3} = \frac{1}{2} \frac{\langle \sigma_{33} \rangle_+^2}{k_3^0 (1-d_3)^2}$$

mode 3 ≡ mode *I*

Note that modes 1, 2 and 3 are here relative to the axes of orthotropy, contrary to the fracture mechanics classical appellation that refers to crack opening directions.

2.1.1 A first choice for the damage evolution law

The evolution of the three damage variables is linked because the same micro-cracks participate to damage. Damage evolution is assumed to be governed by

$$\mathbf{Y} = \sup|_{\tau \le t} (Y_{d3} + \gamma_1 Y_{d1} + \gamma_2 Y_{d2}) \qquad \gamma_1, \gamma_2 \text{ coupling factors}$$

Damage evolution law is

$$\begin{cases} d_3 = w(\mathbf{Y}) & \text{if } d_3 < 1 & d_3 = 1 \text{ otherwise} \\ d_1 = \gamma_1 w(\mathbf{Y}) & \text{if } d_1 < 1 \text{ and } d_3 < 1 & d_1 = 1 \text{ otherwise} \\ d_2 = \gamma_2 w(\mathbf{Y}) & \text{if } d_2 < 1 \text{ and } d_3 < 1 & d_2 = 1 \text{ otherwise} \end{cases}$$

with

$$w(\mathbf{Y}) = \frac{\langle \mathbf{Y} - Y_0 \rangle_+^n}{(Y_c - Y_0)^n}$$

where Y_0 is threshold energy, Y_c is critical energy, n is characteristic parameters of the damage evolution law of the interface.

2.2 Link with fracture mechanics

Classical tests of fracture mechanics[18] allow us to obtain the three inter-laminar fracture toughnesses G_{Ic}, G_{IIc}, G_{IIIc}, relative to the modes I, II and III. G_{Ic}, G_{IIc}, G_{IIIc} are different.[19]

Under the assumption that G_c is a constant parameter (there is no R-curve effect), G_c is a characteristic interface parameter. G_c can be interpreted as the necessary work per unit surface for the interface debonding. Then, it can be dependent (for instance under pure mode I ≡ mode 3) on the characteristic parameters of the interface modelling.

$$G_{Ic} = \int_0^{|u_{3c}|} \sigma_{33} \mathrm{d}[u_3] \qquad \text{with } [u_{3c}] = [u_3]|_{d3=1} \text{: the interface is locally cracked}$$

G_{Ic} is, therefore, the area under the curve $\sigma_{33} - [u_3]$ (see Fig. 2). In pure mode I one finds

$$G_{Ic} = Y_0 + \frac{n}{n+1} (Y_c - Y_0)$$

For the identification under pure modes 2 or 3, one assumes that the crack opening direction coincides with a bisector of adjacent fibre directions. In that case one finds (mode II ≡ mode 1 and mode III ≡ mode 2):

$$G_{\alpha c} = Y_0 \left(\frac{2}{\gamma_i} - 1 \right) + \frac{1}{\gamma_i^{(1/n+1)}} \left(1 - \frac{1}{\gamma_i^{(n+1)}} (Y_c - Y_0) \right) \qquad \text{with } \begin{cases} \alpha = \text{II, III} \\ i = 1, 2 \end{cases}$$

The above relations allow a first identification of damage evolution law parameters.

Note that delamination modelling through an interface with damage includes the notion of process zone given by some authors, because damage varies continually in the vicinity of the crack tip. The process zone length depends on the structure (the damaged zone at the crack tip is different for DCB beams with layers at 0° and 90°).

3 NUMERICAL STRATEGIES

3.1 The boundary layer problem

3.1.1 Problem formulation in elasticity

The laminate shell, of thickness $2h$, occupies the domain $\Omega = \Omega_1 \cup \Omega_2$ (see Fig. 3).

When the thickness $2h$ is weak compared with the transverse dimensions, the three-dimensional displacement–stress solution $(\mathbf{U}, \boldsymbol{\sigma})$ of the elastic problem set on Ω can be written as follows:[20]

$$\begin{cases} \mathbf{U} = \mathbf{U}_P + \mathbf{U}_E \\ \boldsymbol{\sigma} = \boldsymbol{\sigma}_P + \boldsymbol{\sigma}_E \end{cases} \quad \text{with} \quad \begin{cases} (\mathbf{U}_P, \boldsymbol{\sigma}_P)\text{: solution of a shell problem} \\ (\mathbf{U}_E, \boldsymbol{\sigma}_E)\text{: solution localised near the edge } \partial\Omega_2 \end{cases}$$

Notably because of the layer constitutive law discontinuity, the following boundary condition is not respected on the edge $\partial\Omega_2$:

$$\forall z \in [-h, h] \quad \boldsymbol{\sigma}_P(z)\mathbf{n} = \mathbf{F}(z)$$

where $\mathbf{F}$ and $\mathbf{n}$ denote the force density and the normal. Hence $(\mathbf{U}_E, \boldsymbol{\sigma}_E)$ is added to the valid solution far away from the edge $\partial\Omega_2(\mathbf{U}_P, \boldsymbol{\sigma}_P)$ such that $(\mathbf{U}, \boldsymbol{\sigma})$ satisfies the equations and boundary conditions of the three-dimensional problem. $(\mathbf{U}_E, \boldsymbol{\sigma}_E)$ is localised near $\partial\Omega_2$, thus the edge effect solution $(\mathbf{U}_E, \boldsymbol{\sigma}_E)$ can be computed in post-processor of a shell computation set on Ω_2. If, in addition, the radius of curvature of the edge $\partial\Omega_2$ is large compared with the thickness, the variations of $(\mathbf{U}_E, \boldsymbol{\sigma}_E)$ along the tangent direction (y) are negligible, the problem becomes set into a band $\mathscr{B}$ of which the length is in order of the thickness $2h$.

The problem $(\mathscr{P})$ to solve becomes: find $(\mathbf{U}_E, \boldsymbol{\sigma}_E)$

(i) $\mathbf{U}_E \in \mathscr{U} = \{\mathbf{V} / \mathbf{V} = \mathbf{0} \text{ on } \partial\Omega_1 \cap \mathscr{B}\}$

(ii) $\forall \mathbf{V} \in \mathscr{U}, \int_{\mathscr{B}} \boldsymbol{\sigma}_E \boldsymbol{\varepsilon}(\mathbf{V})\, dS = \int_{\partial\Omega_2 \cap \mathscr{B}} \mathbf{R}\mathbf{V}\, ds$

(iii) $\boldsymbol{\sigma}_E = \mathscr{F}(\boldsymbol{\varepsilon}(\mathbf{U}_E))$

The force $\mathbf{R}$ applied on the edge $\partial\Omega_2 \cap \mathscr{B}$ of the structure is the residue of external forces and of the shell solution:

$$\mathbf{R} = \mathbf{F} - \boldsymbol{\sigma}_P \mathbf{n}$$

(i) means that $(\mathbf{U}_E, \boldsymbol{\sigma}_E)$ is localised and (iii) is the constitutive law.

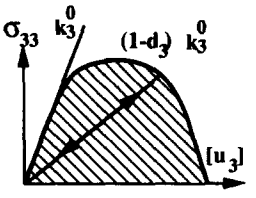

Fig. 2. Interface elastic with damage behaviour (mode I traction).

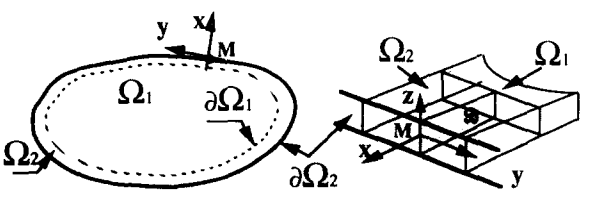

Fig. 3. Boundary layer.

3.1.2 Solving the boundary layer problem in the non-linear case

In the proposed modelling of the laminate, only the interfaces can be damaged due to edge effect normal stresses. The interfaces taking no part in the computation of $(\mathbf{U}_P, \boldsymbol{\sigma}_P)$, it is possible to apply the principle of superimposed stress for the computation of $(\mathbf{U}_E, \boldsymbol{\sigma}_E)$.

The problem $(\mathscr{P})$ to solve becomes a non-linear time dependent problem set into the band $\mathscr{B}$.

We compared the damage states near the free edge obtained by two non-linear computations of a specimen submitted to tension along the x direction (see Fig. 4).

The first computation C_1 has been carried out by resolution of problem $(\mathscr{P})$. The second one C_2 has been a reference computation because it allows us to have the exact three-dimensional solution by searching the displacement under the form proposed by Pipes and Pagano.[22]

$$\mathbf{U}(x, y, z): \begin{cases} u(y, z) + \varepsilon x \\ v(y, z) \\ w(y, z) \end{cases}$$

C_1 and C_2 results are rigorously equal. That confirms it is possible to apply the principle of superimposed stress in that particular case where non-linearities are taken concentrated on interfaces.

3.2 A Riks-like method

Due to damage on interfaces, an instability point may appear. That critical point cannot be passed with a Newton method that pilots the computation in terms of 'force' (see Fig. 5). A Riks-like method[15,16] allows to control the computation and pass such a limit point.

Current step:

$$(\mathscr{S}) \begin{cases} \mathscr{K}_a \delta_i = \lambda_{i+1}\mathbf{F} - \mathbf{f}(\mathbf{U}_i) & \text{By the Newton method: } \delta\lambda_i = 0 \\ \lambda_{i+1} = \lambda_i + \delta\lambda_i & \text{By the Riks method the load factor is released, it is then} \\ \text{constraint: } g(\delta\lambda_i) = 0 & \text{necessary to impose a constraint: } g(\delta\lambda_i) = 0 \end{cases}$$

Riks[15] and Crisfield[16] propose a constraint $g(\delta\lambda_i) = 0$ that concerns the norm of the global vector δ_i. Such a global constraint may lead to a non-convergence when damage localises. To ensure a good convergence we propose to use a local constraint that considers only the more significant degrees of freedom in the increase of damage.

Note α is the closer node of the Gauss point where the increase of damage has been the more important at the initial step (β is the node located on the same interface but on the adjacent layer). n (1, 2 or 3) is the mode of principal damage (see Fig. 6).

The local constraint consists in imposing a constant value for the jump of displacement between α and β along the n direction.

$$(\delta_i)_n^\alpha - (\delta_i)_n^\beta = 0 \qquad \text{for } i \geq 1$$

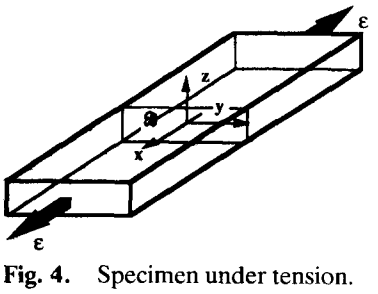

Fig. 4. Specimen under tension.

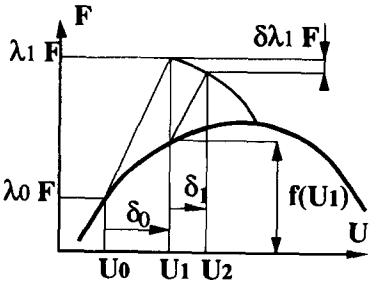

Fig. 5. Riks-like method.

3.3 A method for a large number of layers

The operator $\mathcal{K}_a$ (see $(\mathcal{S})$) can be the tangent structural stiffness matrix $\mathcal{K}_T$ or the secant one $\mathcal{K}_E$ (i.e. computed through an elastic with damage behaviour). Solving $(\mathcal{S})$ can be carried out with the direct Crout method. In the case of a large number of layers, that method may be expensive because of $\mathcal{K}_a$ matrix size. We propose then to use the conjugate gradient method with use of a conditioner.

$$\mathcal{K}_a = \mathcal{K}_E$$

In the iterative Riks algorithm, the linear systems to solve can be written under the form

$$\mathcal{K}_E \mathbf{X} = \mathbf{R} \qquad \text{with } \mathcal{K}_E = \mathcal{K}_{cou} + \mathcal{K}_{int}$$

$\mathcal{K}_{cou}$ and $\mathcal{K}_{int}$ are respectively the contributions of layers ($\mathcal{K}_{cou}$ is a constant matrix) and of interfaces ($\mathcal{K}_{int}$ is a non-constant matrix because the interfaces can damage). The conjugate gradient method consists in a series of iterating resolutions of

$$\mathcal{K}_{cou} \mathbf{Z}_{n+1} = \mathbf{R} - \mathcal{K}_E \mathbf{X}_n$$

The matrix $\mathcal{K}_{cou}$ (conditioner) being diagonal by units, the resolution is parallel on each layer.

4 NUMERICAL SIMULATIONS OF DELAMINATION

4.1 Identification of model parameters

The characteristic parameters of the interface modelling are $k_1^0, k_2^0, k_3^0, Y_0, Y_c, n, \gamma_1, \gamma_2$.

The interface can be considered as a rich resin zone of weak thickness e_1 compared with the layer thickness e_C. By this analogy and by considering that $e_1/e_C \ll 1$, the interface constitutive law can be expressed as

$$\begin{pmatrix} \sigma_{13} \\ \sigma_{23} \\ \sigma_{33} \end{pmatrix} = \begin{pmatrix} k_1^0 & 0 & 0 \\ 0 & k_2^0 & 0 \\ 0 & 0 & k^0 \end{pmatrix} \begin{pmatrix} [u_1] \\ [u_2] \\ [u_3] \end{pmatrix}$$

$$\text{with} \begin{cases} k_1^0 = \dfrac{2G_{13}}{e_1} \\ k_2^0 = \dfrac{2G_{23}}{e_1} \\ k_3^0 = \dfrac{E_3}{e_1} \end{cases} \qquad (1)$$

where G_{13}, G_{23}, E_3: elastic moduli of the rich resin zone, they can be chosen equal to the homogenised layer moduli.

The identification of the other parameters can be carried out by the use of classical fracture mechanics tests[21] results for the mode I (specimen DCB see Fig. 7), the mode II (specimen ENF) and the mode III (specimen SCB). The use of toughness values issued from literature[19] is difficult because those values can present, for the same material (for instance, T300-5208), an important divergence. For the following simulations, we identified the parameters by comparison with experimental results.

4.2 The DCB

We have simulated the DCB test with the EDA program for a comparison with the experimental results[23] (the simulation of the DCB test is not a boundary layer problem).

The studied structure is constituted of 48 layers of thickness $e_C = 0{\cdot}1375$ mm and of T300 fibres with an M10 resin. The numerical simulation has

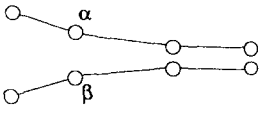

Fig. 6. Concerned nodes by the local constraint.

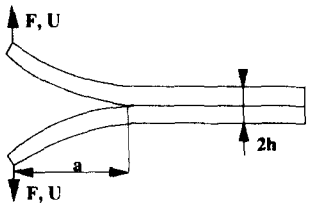

Fig. 7. DCB test.

been carried out with no initial crack, whereas the experimental specimen had an initial crack of 28·5 mm. The authors[23] found $G_{Ic} = 450$ J/m^2 and the following elastic moduli (the elastic moduli relative to the normal direction 3 are supposed to be equal to those in the transverse direction 2).

$$E_{11} = 123\,680 \text{ MPa}$$

$$E_{22} = E_{33} = 8990 \text{ MPa}$$

$$G_{12} = G_{13} = G_{23} = 3770 \text{ MPa}$$

$$\nu_{12} = \nu_{13} = \nu_{23} = 0{\cdot}22$$

We have chosen k_3^0 by eqn. (1):

$$e_I = \frac{e_C}{5} \Rightarrow k_3^0 = 3{\cdot}27 \times 10^8 \text{ MPa/m}$$

Y_0, Y_c, n values satisfy the following relationship:

$$G_{Ic} = Y_0 + \frac{n}{n+1}(Y_c - Y_0) \qquad (2)$$

In view of numerical results, one finds

- the numerical simulation predicts quite well the experimental results since the crack length (simulation) reaches the experimental initial crack length;
- Y_0, Y_c, n values have an influence on the (F, U) curve (see Fig. 8), at the condition these values satisfy eqn (2);
- by the knowledge of the load F associated to the crack length a, it is possible to compute the critical energy release rate G_{Ic} (by the area method[18]).

One finds the experimental value of G_{Ic} and one verifies that the critical energy release rate is independent of the crack length (see Fig. 9). This result has been verified experimentally[23] and theoretically established[14] for an initial crack which is large compared with the thickness $2h$. The important point is the numerical simulation predicts this result even if the crack length is short.

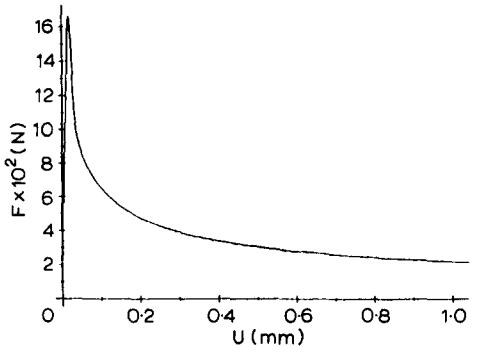

Fig. 8. F–U curve.

4.3 Delamination near the free edge of a specimen under tension or compression

We compared our simulations of delamination near the free edge of a specimen under tension or compression (see Fig. 4) with first experimental results[5,24] for mode I delamination (on the mid-plane interface) of a T300-5208 material (see Table 1). Then, we also compared our results with experimental ones[25] for mixed mode of delamination of a T300-1034C (see Table 2). The

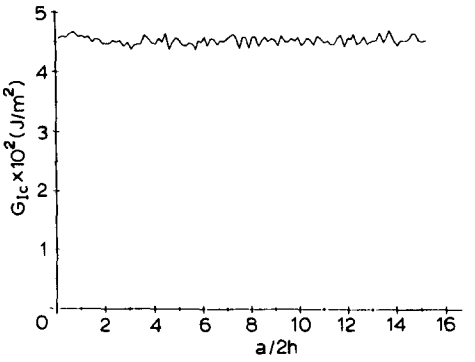

Fig. 9. G_{Ic}–a curve.

Table 1. Mode I delamination[a]

Laminate	ε_{exp}	ε_{cal}
$(\pm 45, 0, 90)_s$	0·53	0·53
$(\pm 45_2, 0_2, 90_2)_s$	0·45	0·38
$(\pm 45_3, 0_3, 90_3)_s$	0·36	0·32
$(0, \pm 45, 90)_s$	0·66	0·61
$(45, 0, -45, 90)_s$	0·54	0·57
$(\pm 30, 90)_s$	0·39	0·43
$(\pm 30_2, 90_2)_s$	0·36	0·39

[a]Data taken from Refs 5 and 23.

Table 2. Mixed mode delamination[a]

Laminate	Interface	ε_{exp}	ε_{cal}
$(\pm 45, 90, 0)_s$	90, 0	0·71	0·77
$(90_4, \pm 30_4)$	30, −30	−0·27	−0·28
$(90_4, \pm 15_4)$	15, −15	−0·34	−0·36
$(0_2, \pm 30_2)_s$	30, −30	−0·54	−0·65
$(0_4, \pm 30_4)_s$	30, −30	−0·35	−0·4
$(0_4, \pm 30_4)_s$	30, −30	0·85	0·73
$(0_2, \pm 15_2)_s$	15, −15	−0·51	−0·6
$(0_4, \pm 15_4)_s$	15, −15	−0·35	−0·45
$(0_4, \pm 15_4)_s$	15, −15	0·57	0·5

[a]Data taken from Ref. 25.

authors[5,25] propose the same elastic moduli for both materials T300-5208 and T300-1034C.

$$E_{11} = 138\,000 \text{ MPa}$$

$$E_{22} = E_{33} = 9700 \text{ MPa}$$

$$G_{12} = G_{13} = G_{23} = 5500 \text{ MPa}$$

$$\nu_{12} = \nu_{13} = 0{\cdot}3,\ \nu_{23} = 0{\cdot}6$$

We have chosen the interface stiffnesses by eqn (1) and $e_1 = e_C/5$.

First, we have identified under mode I (T300-5208) the parameters Y_c, Y_0 and n with the $(\pm 45, 0, 90)_s$ laminate. Secondly, we have identified the parameters γ_1 and γ_2 under mixed mode (T300-1034C) such that the results are quite good. So, we assumed that both T300-5208 and T300-1034C damage behaviours were close.

The calculated strain (ε_{cal}) in the tables corresponds to the maximum of strain of the strain-crack length curve (see Fig. 10).

5 CONCLUSION

The analysis of delamination near an edge of a laminate structure by damage mechanics has been presented. The basic assumptions of this method — the edge is quasi-straight, damage is taken concentrated on interfaces between layers — lead to a simplified method for the delamination onset and propagation forecast. The identification of characteristic parameters of the interface modelling can be carried out by use of classical fracture mechanics tests. The finite element program EDA is independent of finite element codes, it acts as a post-processor of an elastic laminate shell computation. Note there is no mesh dependency because the treated problem is plane and damage is concentrated on interfaces. The first comparisons of numerical simulations with experimental results are quite good.

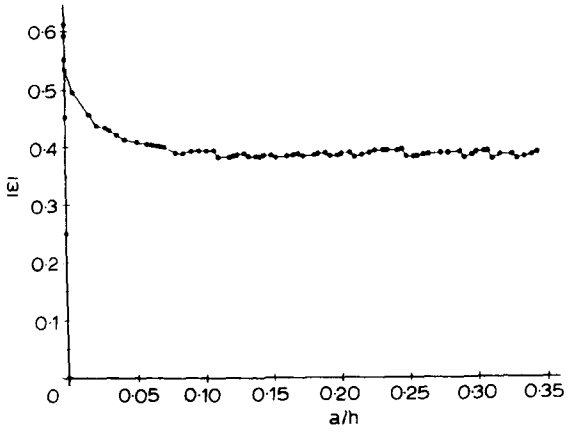

Fig. 10. ε–a curve for a $(0, \pm 45, 90)_s$ laminate: delamination on the mid-plane interface.

REFERENCES

1. Tsai, S. W. & Wu, E., A general theory of strength for anisotropic materials. *J. Comp. Mater.*, **5** (1971) 58–80.
2. Engrand, D., A boundary layer approach to the calculation of transverse stresses along the free edges of a symmetric laminated plate of arbitrary width under in plane loading. *Comp. Structures*, (1981) 247–61.
3. Dumontet, H., Study of a boundary layer problem in elastic composite materials, *M²AN*, **20** (1986) 265–86.
4. Bar-Yoseph, P., On the accuracy of interlaminar stress calculation in laminated plates. *Comp. Meth. Appl. Mech. Eng.*, **36** (1983) 309–29.
5. Kim, R. Y. & Sony, S. R., Experimental and analytical studies on the onset of delamination in laminated composites. *J. Comp. Mater.*, **18** (1984) 70–6.
6. Wang, A. S. D., Fracture analysis of interlaminar cracking. *Interlaminar Response of Composite Materials* (Composite Material Series, Vol. 5), ed. N. J. Pagano. Elsevier Science Publishers, 1989, pp. 69–109.
7. Wang, A. S. D., Slomania, M. & Bucinell, R. B., Delamination crack growth in *Composite Laminates, Delamination and Debonding of Materials*, ed. W. S. Johnson. ASTM STP876, Washington, DC, USA, 1985, pp. 135–67.
8. O'Brien, T. K., Characterisation of delamination onset and growth in a composite laminate, *Damage in Composite Materials*, ed. K. L. Reifsnider. ASTM-STP775, Washington, DC, USA, 1982, pp. 140–67.
9. Talreja, R., Damage development in composites: mechanisms and modelling. *J. Strain Anal.*, **24** (1989) 215–22.
10. Allen, D. H., Groves, S. E. & Harris, C. E., A cumulative damage model for continuous fibre composite laminates with matrix cracking and interply delaminations, *Composite Materials: Testing and Design*, ed. J. D. Withcomb. ASTM-STP972, Washington, DC, USA, 1988, pp. 57–80.
11. Ladevèze, P., Allix, O. & Daudeville, L., Mesomodelling of damage for laminate composites: application to delamination. In *IUTAM Symposium on Inelastic Deformation of Composites Materials, Troy*, ed. G. J. Dvorak. Springer-Verlag, 1990, pp. 607–22.
12. Allix, O., Daudeville, L. & Ladevèze, P., Delamination and damage mechanics, *Mechanics and Mechanism of Damage in Composites and Multi-Materials*, ed. D. Baptiste. ESIS Publication 11, London, UK, 1991, pp. 32–41.
13. Schellekens, J. C. J. & De Borst, R., Numerical simulation of free edge delamination in graphite epoxy specimen under uniaxial extension. In *Sixth International Conf. on Composite Structures ICCS6*, ed. I. H. Marshall. Elsevier Science Publishers, 1991, pp. 647–57.
14. Allix, O. & Ladevèze, P., Interlaminar interface modelling for the prediction of delamination. *Comp. Structures*, **22** (1992) 235–42.
15. Riks, E., An incremental approach to the solution of snapping and buckling problems. *Int. J. Solids and Structures*, **15** (1979) 524–51.

16. Crisfield, M. A., An arc-length method including line searches and accelerations. *Int. J. Num. Methods Eng.*, **19** (1983) 1269–89.
17. Corigliano, A., Formulation, identification and use of interface models in the numerical analysis of composite delamination. Submitted to *Int. J. Solids and Structures*, 1992.
18. Whitney, J. M., Experimental characterisation of delamination fracture. In *Interlaminar Response of Composite Materials* (Composite Material Series, Vol. 5), ed. N. J. Pagano. Elsevier Science Publishers, 1989, pp. 161–250.
19. Sela, N. & Ishai, O., Interlaminar fracture toughness and toughening of laminated composite materials: a review. *Composites*, **20** (1989) 423–35.
20. Nesa, A., Abisror, A. & Bunsell, A. R., On cracking in a unidirectional glass-epoxy composite: toughness and damage mechanisms.
21. Fredrichs, K. O. & Dressler, R. F., A boundary layer theory for elastic plates. *Comm. Pure and Appl. Math.*, **14** (1961) 1–33.
22. Pipes, R. B. & Pagano, N. J., Interlaminar stresses in composite laminates under axial extension. *J. Comp. Mater.*, **4** (1970) 538–48.
23. Laksimi, A., Benzeggagh, M. L., Jing, G., Hecini, M. & Roelandt, J. M., Mode I interlaminar fracture of symmetrical cross-ply composites. *Comp. Sci. Technol.*, **41** (1991) 147–64.
24. Rodini, B. T. & Eisenman, J. R., An analytical and experimental investigation of edge delamination in composite laminates. In *Proc. 4th Conf. Fibrous Comp. San Diego*, ed. Lenoe & Oplinger & Burke, 1978, pp. 441–57.
25. Kim, R. Y. & Sony, S. R., *Delamination of Composite Laminates Stimulated by Interlaminar Shear.* ASTM-STP893, Washington, DC, USA, 1986, pp. 286–307.